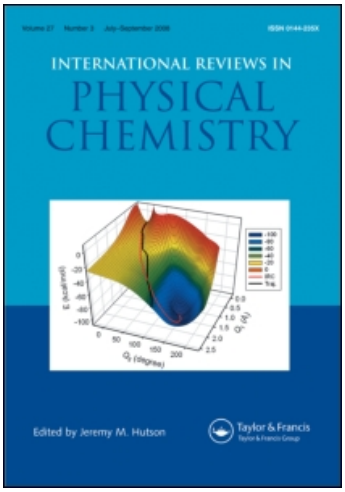

International Reviews in Physical Chemistry
Publication details, including instructions for authors and subscription information:
http://www.informaworld.com/smpp/title~content=t713724383

Probing the intermediates in the MO + CH_4 ↔ M + CH_3OH reactions by matrix isolation infrared spectroscopy

Guanjun Wang[a]; Mingfei Zhou[a]
[a] Department of Chemistry, Shanghai Key Laboratory of Molecular Catalysts and Innovative Materials, Advanced Materials Laboratory, Fudan University, Shanghai 200433, P.R. China

To cite this Article Wang, Guanjun and Zhou, Mingfei(2008) 'Probing the intermediates in the MO + CH_4 ↔ M + CH_3OH reactions by matrix isolation infrared spectroscopy', International Reviews in Physical Chemistry, 27: 1, 1 — 25
To link to this Article: DOI: 10.1080/01442350701685946
URL: http://dx.doi.org/10.1080/01442350701685946

International Reviews in Physical Chemistry
Vol. 27, No. 1, January–March 2008, 1–25

Taylor & Francis
Taylor & Francis Group

Probing the intermediates in the $MO + CH_4 \leftrightarrow M + CH_3OH$ reactions by matrix isolation infrared spectroscopy

Guanjun Wang and Mingfei Zhou*

Department of Chemistry, Shanghai Key Laboratory of Molecular Catalysts and Innovative Materials, Advanced Materials Laboratory, Fudan University, Shanghai 200433, P.R. China

(*Received 1 August 2007; final version received 14 September 2007*)

In this review, we present our recent studies on the $MO + CH_4$ and $M + CH_3OH$ model reactions (M = transition metals) in order to provide quantitative information regarding the mechanisms for the catalytic methane-to-methanol conversion process. The reaction intermediates were trapped and probed by matrix isolation infrared absorption spectroscopy. Various important intermediates including $OM(CH_4)$, $M(CH_3OH)$, CH_3MOH, $CH_3M(O)H$ and CH_3OMH are identified *via* isotopic substitution experiments in the $MO + CH_4$ and $M + CH_3OH$ reactions for selected early and late transition metals. Based on the observed reaction intermediates, some unprecedented reaction pathways are proposed. Complementary quantum chemical calculations support the intermediate identification and help to gain insight into the reaction mechanisms and periodic trends.

Keywords: reaction intermediate; methane-to-methanol conversion; matrix isolation; transition metal; reaction mechanism

Contents

*Corresponding author. Email: mfzhou@fudan.edu.cn

ISSN 0144–235X print/ISSN 1366–591X online

DOI: 10.1080/01442350701685946
http://www.informaworld.com

1. Introduction

The conversion of methane to more easily handled products such as methanol is of great economic and scientific importance.[1–3] Although the oxidation reaction, $CH_4 + 1/2O_2 \rightarrow CH_3OH$ is thermodynamically favoured, no direct efficient methane-to-methanol conversion scheme has yet been developed[4]. The development of catalysts for selective oxidation of methane to methanol under mild conditions is a great challenge and has attracted intensive experimental and theoretical interest. A lot of transition-metal derived catalysts have been developed for the controlled oxidation of methane, including some heterogeneous catalysts,[5–7] homogeneous catalysts[8,9] and enzyme catalysts.[10] While the catalytic processes consist of a complicated sequence of interrelated reactions, the investigation of the $MO^+ + CH_4 \rightarrow M^+ + CH_3OH$ and $MO + CH_4 \rightarrow M + CH_3OH$ reactions and their reverse reactions can potentially provide quantitative information regarding the thermodynamics and mechanisms for the catalytic methane-to-methanol conversion processes. Such model reactions can be studied under well-defined conditions, and free of effects from ligand, solvent, surface active site and crystal lattice.

The reactions of gas phase transition metal monoxide cations with methane have been extensively studied both experimentally[11–23] and theoretically.[23–32] Schwarz and coworkers have systematically studied the gas phase reactions of the transition metal monoxide cations and methane using different experimental techniques including ion cyclotron resonance and guided ion beam mass spectrometry.[16–23] The product distributions and energetics were measured. The results of these studies show that the late transition metal monoxide cations are able to convert methane to methanol, but the efficiency depends strongly on the metals. For example, MnO^+ reacts with methane very efficiently, but the branching ratio in forming methanol is less than 1%.[20] FeO^+ also efficiently reacts with methane at thermal energies, the yield of methanol is 41%.[16] CoO^+ exhibits low reactivity toward methane, but the branching ratio in forming methanol is 100%.[18] The early transition metal monoxide cations are unreactive toward methane due to the strong bonding interaction between metal and oxygen. In contrast, the metal cations are able to react with methanol to form metal monoxide cation and methane in the gas phase.[33] Based on the final product analysis, the $MO^+ + CH_4 \rightarrow M^+ + CH_3OH$ reactions were suggested

to proceed *via* an important $[CH_3MOH]^+$ intermediate. A more detailed mechanism has been developed based upon theoretical calculations.[24–32] The reactions were suggested to proceed *via* the initial formation of a $[OM(CH_4)]^+$ complex followed by the isomerization to the $[CH_3MOH]^+$ and $[M(CH_3OH)]^+$ intermediates *via* two transition states. The results showed that the experimentally observed reaction efficiency and methanol-to-methyl branching ratio could be rationalized in terms of the predicted barrier heights at the transition states.[30] Although the proposed reaction intermediates on the potential energy surfaces were not directly observed in the mass spectrometric study of the $MO^+ + CH_4 \rightarrow M^+ + CH_3OH$ reactions in the gas phase, four distinct intermediates with $FeCH_4O$ stoichiometry were generated by Schwarz and coworkers in a clean fashion by reacting Fe^+ with appropriate organic precursors in an ion cyclotron resonance cell and were characterized by using collisional activation mass spectrometry.[34] The $[CH_3FeOH]^+$ and $[H_2OFeCH_2]^+$ intermediates were also produced by specific ion molecule reactions, cooled in a supersonic expansion, and their photodissociation spectra were measured by Metz and coworkers.[35,36]

In contrast to the cation reaction systems, the neutral $MO + CH_4 \rightarrow M + CH_3OH$ reactions and reverse reactions have gained much less attention, in part because of the experimental challenges faced in detecting neutral species in the gas phase. While the mass spectrometry is sensitive in detecting charged species, it is nearly blind to the neutral species. The fast flow tube reactor is the most commonly used technique applied to the study of neutral metal atom reactions in the gas phase.[37,38] Some spectroscopic techniques such as laser induced fluorescence were employed to detect the metal atoms for estimating their concentrations, and hence, kinetic information such as reaction rate can be calculated. However, it is difficult to produce a clean neutral transition metal monoxide source for reaction study using the flow tube technique. Matrix isolation is a very commonly used technique in the investigation of neutral metal atom reactions.[39–41] Matrix isolation coupled with spectroscopic techniques such as infrared absorption has proven to be a powerful method for delineating reaction mechanisms by facilitating the isolation and characterization of the reactive intermediates.[42–44] Particularly relevant to the topic of this review, the reactions of transition metal atoms with methane have been intensively studied by matrix isolation infrared spectroscopy.[45–67] Various intermediates such as $HMCH_3$, $H_2C{=}MH_2$ and $HC{\equiv}MH_3$ were trapped and identified, which are very helpful in understanding the mechanism of C–H bond activation of saturated alkanes by transition metal centres.

In this review, we summarize our recent progress in understanding the mechanism of methane-to-methanol conversion by transition metal monoxide neutrals. We focus on trapping and identification of the potentially important intermediates involved in the conversion process using matrix isolation infrared absorption spectroscopy. Both the reactions of metal atoms with methanol and metal monoxide molecules with methane were investigated. Several early transition metal as well as late transition metal systems were studied to elucidate the periodic trends.

This review is organized as follows. The experimental approach and theoretical method are described in the next section. The results on the $MO + CH_4$ reactions are presented in Section 3, while the $M + CH_3OH$ reactions are summarized in Section 4. The vibrational frequencies for the experimentally observed reaction intermediates are presented in Section 5. Finally, some conclusions are given in Section 6.

2. Experimental approach and theoretical method

2.1. *Experiment apparatus*

The experiments were performed by using pulsed laser ablation-matrix isolation infrared absorption spectroscopy. The transition metal atoms and monoxide molecules were prepared by pulsed laser ablation of bulk metal or metal oxide targets. Laser ablation has been widely used to produce reactive intermediates and radicals for gas phase jet studies as well as low temperature matrix isolation spectroscopic studies.[39,40,68] It has also proved to be a convenient method to produce atoms from a solid for matrix isolation studies. In contrast to conventional thermal evaporation techniques, with laser ablation only a small amount of the material is directly heated, thus minimizing the introduction of impurities into the sample and the heat load on the matrix, particularly for transition metals which have a very high melting point temperature. The preparation of transition metal monoxide neutrals is more difficult than the production of transition metal atoms. Most transition metals exhibit several oxidation states, and hence, the species evaporated from the bulk metal oxide target usually is a mixture composed of oxides with different oxidation states. We were able to prepare relatively 'pure' transition metal monoxides by laser ablation of selected metal oxide targets with controlled laser energy for some transition metals.

A schematic diagram of the apparatus is shown in Figure 1, which is similar to those used previously in the literature.[69,70] The 1064 nm Nd:YAG laser fundamental (Spectra Physics, DCR 150, 20 Hz repetition rate and 8 ns pulse width) was focused onto a rotating bulk metal or metal oxide target. The laser ablated metal atom or metal oxide species were co-deposited with reagent gas in excess argon onto a cooled CsI window, which is maintained at 6 K by means of a closed-cycle helium refrigerator. The samples were usually deposited (accumulated) for one to three hours. The laser evaporated species may involve excited species and electrons and ions. If these high energy species are involved in

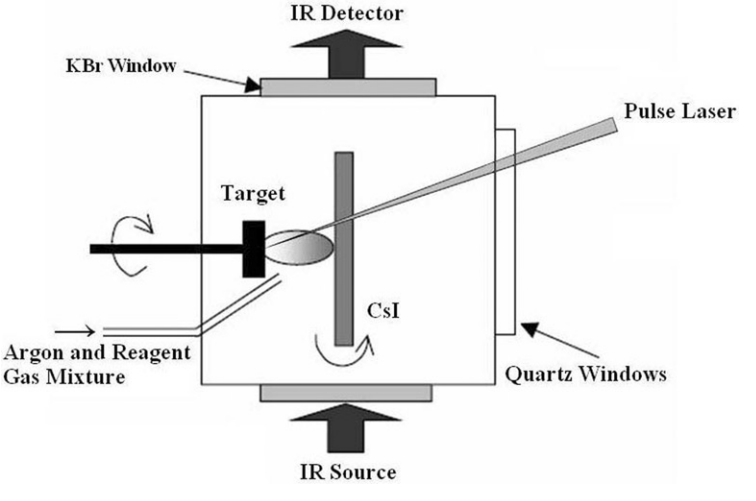

Figure 1. Schematic diagram of apparatus for laser ablation matrix isolation infrared spectroscopic investigation of intermediates in the $MO + CH_4$ and $CH_3OH + M$ reactions.

the reactions, the identification of the reaction intermediates and products and reaction pathways can be problematic. Therefore, we use relatively low ablation laser energy, so that the ablated species can be efficiently quenched and reactions during sample deposition are largely avoided. With the use of low laser energy, the possibility for the formation of clusters can also be avoided, therefore, the atomic reactions dominate the chemistry. After deposition, the samples were annealed to allow the trapped reactants to diffuse and react. The reaction can be very effectively quenched after the primary reaction, and the energy-rich intermediates which fragment readily in the gas phase may be stabilized in detectable concentration in solid matrix. Selected samples were also subjected to broad-band irradiation using a tungsten lamp or a high-pressure mercury arc lamp with glass filters to initiate further isomerization or dissociation reactions. The infrared absorption spectra of the intermediates and products in the middle infrared region (4000–400 cm^{-1}) were recorded on a Bruker IFS 113V spectrometer at 0.5 cm^{-1} resolution using a DTGS or liquid nitrogen cooled MCT detector. The vibrational absorptions of intermediates and products were assigned based on isotopic substitution experiments. Isotopic labelled CD_4 (Isotec, 99%),$^{13}CH_4$ (Isotec, 99%), $^{13}CH_3OH$, $CH_3{}^{18}OH$ and CH_3OD (Isotec, 99%) samples and mixtures were used in different experiments.

2.2. *Theoretical method*

In order to validate the experimental assignments and to gain a detailed understanding of the reaction mechanism, quantum chemical calculations were performed. This involves calculations not only of the equilibrium geometries and vibrational spectra of the intermediates and products experimentally detected, but also energetics and potential energy surfaces. In some cases, both the ground state and excited state potential energy surfaces were calculated. The evaluation of accurate molecular properties and energetics usually needs sophisticated high level *ab initio* calculations. However, it is very difficult to compute the transition metal-containing systems with high level *ab initio* methods. Density functional theory (DFT) provides a good prediction of the geometries, vibrational frequencies and energetics of mononuclear transition metal compounds.[71–73] All calculations were performed using the Gaussian program.[74] The three-parameter hybrid functional according to Becke with additional correlation corrections due to Lee, Yang, and Parr (B3LYP) was utilized.[74,75] The 6-311++G(d, p) or 6-311++G(3df, 3pd) basis set was used for the H, C and O atoms. The all-electron basis sets of Wachter and Hay as modified by Gaussian were used for the first row transition metals, and the SDD pseudopotential and basis sets were used for the second and third row transition metals.[76–78] Reactants, various possible intermediates and transition states and products were optimized. The geometries were fully optimized, and the stability of the electronic wave function was tested; the harmonic vibrational frequencies were calculated with analytic second derivatives, and zero-point energies (ZPE) were derived. The single-point energies of selected structures optimized at the B3LYP level were calculated using the CCSD(T) method.[79] Transition state optimizations were done with the synchronous transit-guided quasi-Newton (STQN) method.

3. The MO + CH_4 reactions

The reactions of neutral transition metal monoxides with methane have not been reported experimentally, but have been the subject of some theoretical calculations. Broclawik *et al.*[80,81] have investigated the interaction of palladium monoxide with methane by means of density functional theory, and found that palladium monoxide can form a weak complex bound by 3.3 kcal/mol. The insertion of PdO into the C–H bond of methane to form CH_3PdOH was predicted to have an energy barrier of 24.5 kcal/mol. The reactions of scandium, nickel, and palladium monoxides with methane were also studied by Hwang and Mebel using density functional calculations.[82,83] Similar to the transition metal monoxide ions, neutral NiO and PdO are reactive toward methane and can form molecular complexes with CH_4 bound by 8–9 kcal/mol without a barrier. At elevated temperatures, the dominant reaction channel is direct abstraction of a hydrogen atom by the oxides from CH_4 with a barrier of 16 kcal/mol. The insertion into a C–H bond to produce CH_3MOH is a minor reaction channel and proceeds *via* a transition state lying 19–20 kcal/mol above the initial reactants. On the contrary, the results showed that ScO is not reactive with respect to methane at low and ambient temperatures. Goddard and coworkers investigated the methane activation by MO_x (M = Cr, Mo, W; $x = 1, 2, 3$), and found that the trends in reactivity can be rationalized in terms of changes in electrophilicity of MO_x, the strength of the M–O π bonds, and the binding properties of MO_x to methyl or hydrogen.[84] These theoretical studies have provided valuable information concerning the reaction mechanism and energetics.

We performed matrix isolation spectroscopic studies on the reactions of transition metal monoxides with methane. The study is mainly focused on the first row transition metals. We were not able to prepare a considerable quantity of isolated VO in the matrix, therefore, niobium and tantalum monoxides were selected as the congener candidate.

3.1. *FeO, MnO + CH_4 reactions*

The reactions of MnO and FeO with methane are similar.[85] The monoxide reactants were prepared by laser ablation of bulk MnO_2 and Fe_2O_3 targets. Under controlled laser energy, the monoxide is the dominate species from laser ablation. The spectra in selected regions with a MnO_2 target are shown in Figure 2. It was found that the manganese and iron monoxides reacted with methane spontaneously on annealing to form the $OMn(CH_4)$ and $OFe(CH_4)$ complexes. The $OMn(CH_4)$ complex was predicted to have a $^6A_1$ ground state, while the $OFe(CH_4)$ complex a $^5A_1$ ground state, both of which correlate to the ground state of metal monoxides. The complexes have a C_{2V} symmetry with the metal atom coordinated to two hydrogen atoms of the methane molecule, as shown in Figure 3. The $OMn(CH_4)$ and $OFe(CH_4)$ complexes were predicted to be bound by 1.9 and 4.8 kcal/mol respectively, with respect to $MnO + CH_4$ and $FeO + CH_4$ at the B3LYP/6-311++G** level of theory after zero point energy corrections. These values are significantly smaller than those for the corresponding monoxide cations (16.2 and 22.8 kcal/mol for MnO^+ and FeO^+)[25–27] and are even smaller than those of NiO and PdO (9–10 kcal/mol).[83,84]

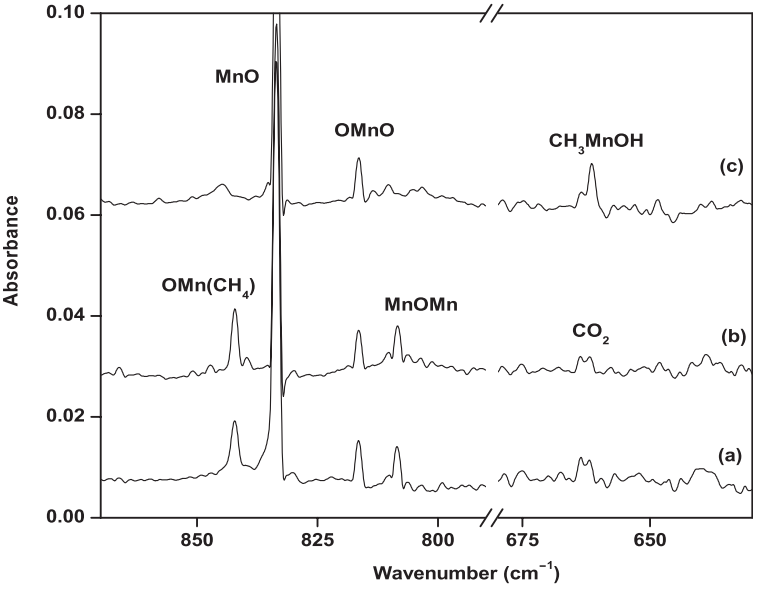

Figure 2. Infrared spectra in selected regions from co-deposition of laser-ablated MnO_2 target with 0.8% CH_4 in excess argon. (a) 2 h of sample deposition at 12 K; (b) after 30 K annealing; (c) after 30 min of broad-band ($250 < \lambda < 580$ nm) irradiation. From ref. 85.

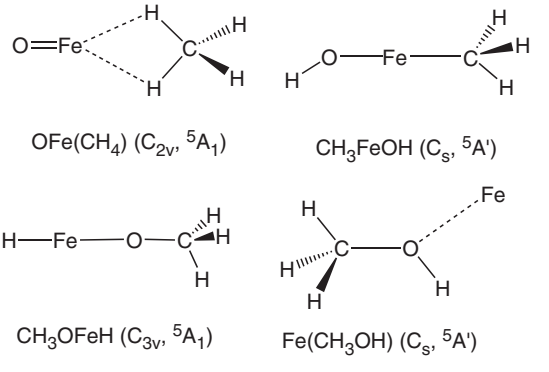

Figure 3. Optimized structures (B3LYP/6-311++G**) of the intermediates in the $FeO + CH_4 \rightarrow Fe + CH_3OH$ reaction. From ref. 85.

The $OMn(CH_4)$ and $OFe(CH_4)$ complexes rearrange to the CH_3MnOH and CH_3FeOH isomers under UV light irradiation with the wavelength range of 250–300 nm. According to DFT/B3LYP calculations, the CH_3MnOH and CH_3FeOH molecules are 39.3 and 36.8 kcal/mol lower in energy than the $OMn(CH_4)$ and $OFe(CH_4)$ complexes, respectively. The formation of CH_3MOH is a photochemical process, and most likely involves an electronically excited state of essentially MO, which is only weakly perturbed by the methane ligand.

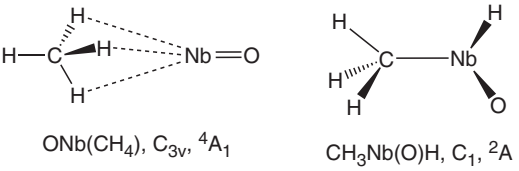

Figure 4. Optimized structures of the intermediates observed in the $NbO + CH_4$ reaction at the B3LYP/6-311++G**/SDD level of theory. From ref. 86.

3.2. *NbO, TaO + CH_4*

The niobium and tantalum monoxides were prepared by laser-evaporation of the bulk Nb_2O_5 and Ta_2O_5 targets.[86] The NbO molecule reacted with methane spontaneously to form the $ONb(CH_4)$ complex, which has a $^4A_1$ ground state with a C_{3v} symmetry (Figure 4). The niobium atom of NbO is coordinated to three hydrogen atoms of CH_4, i.e. η^3–CH_4 bonding. The $^4A_1$ state correlates to the ground state NbO ($^4\sum^-$) and CH_4, and is very weakly bound. The binding energy of $ONb(CH_4)$ was predicted to be only 0.9 kcal/mol with respect to NbO ($^4\sum^-$) + CH_4 calculated at the CCSD(T)/B3LYP/6-311++G**/SDD level. The TaO molecule has a doublet ($^2\Delta$) ground state. It may interact with methane to form the $OTa(CH_4)$ complex, which was predicted to have a ^2E ground state with a C_{3v} symmetry, analogous to $ONb(CH_4)$. The binding energy was computed to be 1.0 kcal/mol at the CCSD(T)/B3LYP/6-311++G**/SDD level. No $OTa(CH_4)$ absorptions were observed in the experiments. We assume that the $OTa(CH_4)$ complex was formed, but its absorptions were overlapped by the strong CH_4 and TaO absorptions.

The $ONb(CH_4)$ and $OTa(CH_4)$ complexes rearrange to the $CH_3Nb(O)H$ and $CH_3Ta(O)H$ isomers upon $300 < \lambda < 580$ nm irradiation. Both $CH_3Nb(O)H$ and $CH_3Ta(O)H$ were predicted to have a doublet ground state without any symmetry, as shown in Figure 4. They can be regarded as being formed *via* a hydrogen atom transfer from methane to the metal centre. The $CH_3Nb(O)H$ and $CH_3Ta(O)H$ structures are about 27.6 and 29.0 kcal/mol more stable than the $ONb(CH_4)$ and $OTa(CH_4)$ complexes, respectively.

Besides metal monoxides, laser evaporation of bulk Nb_2O_5 and Ta_2O_5 targets also produced metal dioxides (NbO_2 and TaO_2), which also reacted with methane to form the $O_2Nb(CH_4)$ and $O_2Ta(CH_4)$ complexes. Both complexes have a $^2A'$ ground state with a C_s symmetry. They photochemically rearranged to the more stable $CH_3Nb(O)OH$ and $CH_3Ta(O)OH$ isomers *via* one hydrogen atom transfer from methane to one of oxygen atom of metal dioxide, as shown in Scheme 1.

3.3. *TiO + CH_4*

The TiO molecule was generated by pulsed laser ablation of bulk titanium dioxide target. The spectra in a selected region from the $TiO + CH_4$ reaction are shown in Figure 5. From the spectra, the $TiO + CH_4$ reaction can be summarized as Scheme 2.[87]

The initial step of the reaction between titanium monoxide and methane is also the formation of the 1:1 complex. In contrast to other previously reported transition metal

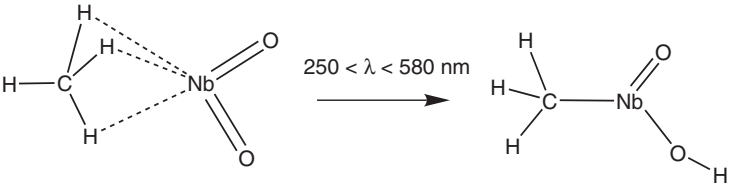

Scheme 1. The reaction from $O_2Nb(CH_4)$ to $CH_3Nb(O)H$.

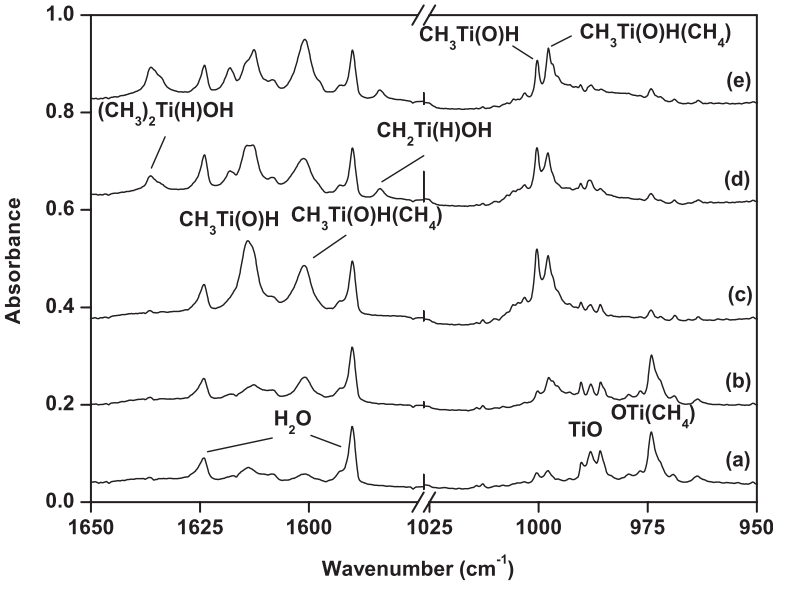

Figure 5. Infrared spectra in the Ti–H and Ti=O stretching frequency regions from the reactions of TiO with 5.0% CH_4 in argon. (a) After 3 h of sample deposition at 12 K; (b) after 30 K annealing; (c) after 30 min of $\lambda > 500$ nm irradiation; (d) after 30 min of $\lambda > 250$ nm irradiation; and (e) after 35 K annealing. From ref. 87.

monoxide–methane complexes, which were predicted to be coordinated between the metal and H atoms, the $OTi(CH_4)$ complex was predicted to have a C_{3v} structure with one of H atom of CH_4 coordinated to the O atom of TiO, as shown in Figure 6. The small deformation of the CH_4 and TiO subunits and the rather long O–H distance (2.658 Å calculated at the B3LYP level) indicate weak interaction between the CH_4 and TiO subunits. The binding energy with respect to $TiO + CH_4$ was predicted to be 1.1 kcal/mol at the CCSD(T)//B3LYP level, significantly lower than those of late transition metal monoxide–methane complexes. From the complex, one hydrogen atom of methane transferred to the metal centre to form the $CH_3Ti(O)H$ molecule under $\lambda > 500$ nm light irradiation. The $CH_3Ti(O)H$ molecule was predicted to have a singlet ground state with a non-planar C_1 structure (Figure 6). The calculated Ti–C bond length of 2.088 Å suggests a Ti–C single bond, which is very close to the standard single Ti–C bond lengths in

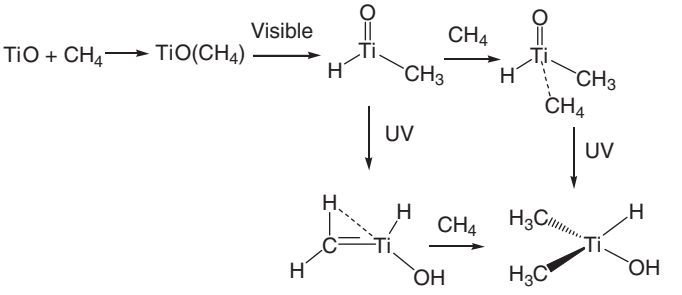

Scheme 2. The mechanism for the $TiO + CH_4$ reaction.

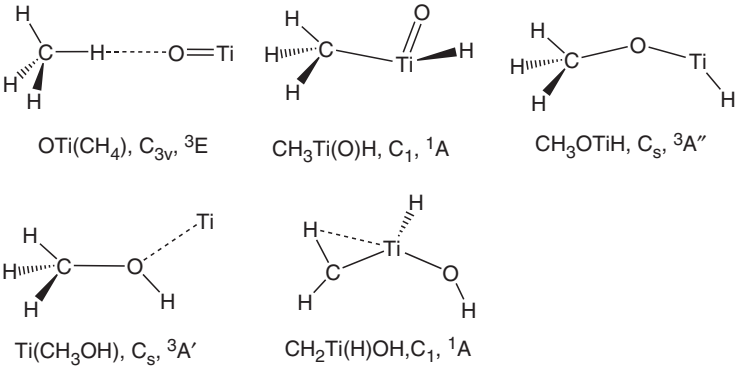

Figure 6. Optimized structures of the intermediates observed in the $TiO + CH_4$ reaction at the B3LYP/6-311++G** level of theory. From ref. 87.

tetraaryl compounds.[88] The $CH_3Ti(O)H$ molecule can be regarded as a titano-acetaldehyde. According to the calculations, the singlet ground state $CH_3Ti(O)H$ molecule is 6.9 kcal/mol lower in energy than the triplet state $OTi(CH_4)$ complex. The H atom transfer process is thus exothermic but requires activation energy. This isomerization process involves spin crossing and proceeds only under visible light ($\lambda > 500$ nm) irradiation, during which some excited states may be involved. No absorptions due to the CH_3TiOH structure were experimentally observed. This structure was predicted to be 3.7 kcal/mol higher in energy than the $CH_3Ti(O)H$ isomer.

Under UV light ($\lambda > 250$ nm) irradiation, one hydrogen atom of CH_3 group can further be transferred to the O atom in $CH_3Ti(O)H$ to form the $CH_2Ti(H)OH$ isomer. The $CH_2Ti(H)OH$ molecule has a singlet ground state with a non-planar C_1 structure, as illustrated in Figure 6. The Ti–C bond length of 1.815 Å is slightly shorter than the experimentally known Ti=C double bond length.[89,90] The $CH_2Ti(H)OH$ molecule is a methylidene hydrido hydroxide complex, which can also be regarded as a titano-vinyl alcohol molecule. Similar to the recently reported methylidene hydride $CH_2{=}MH_2$[57–62] and the fluorine substituted derivatives $CH_2{=}MHF$ (M = Ti, Zr, Hf, Mo and W),[91,92] the

$CH_2Ti(H)OH$ titano-vinyl alcohol molecule involves agostic interaction between the metal atom and one of the α-hydrogen atoms.[93] The methylene group is distorted with one of the methylene hydrogen atoms located close to the Ti atom: $\angle HCTi = 89.1^\circ$ and $r_{CH\ldots Ti} = 2.117$ Å. The $CH_2Ti(H)OH$ structure is 23.4 kcal/mol less stable than the ground state $CH_3Ti(O)H$ isomer. The reaction on the singlet ground state was computed to proceed *via* a transition state lying 51.4 kcal/mol above $CH_3Ti(O)H$. A similar ultraviolet induced alpha-H transfer has been observed for CH_3TiX to form CH_2TiHX (X = H, F) in the reactions of Ti atoms with CH_4 and CH_3F.[57,92]

It was found that $CH_2Ti(H)OH$ further reacted with a second methane to form titano-isopropyl alcohol, $(CH_3)_2Ti(H)OH$ on annealing, which suggests that $CH_2Ti(H)OH$ is able to activate methane with very low activation energy. The activation process is predicted to be exothermic by about 32.1 kcal/mol. The reaction proceeds with the initial formation of a $CH_2Ti(H)OH(CH_4)$ complex followed by a hydrogen atom transfer *via* a transition state lying 4.0 kcal/mol above the $CH_2Ti(H)OH + CH_4$ reactants. The energy barrier is quite low and tunnelling effects which are common for hydrogen atom transfer reactions might be responsible for the formation of $(CH_3)_2Ti(H)OH$ on annealing.[94,95]

Experiments were also performed on other first row transition metal monoxides. ScO reacted with methane to form the $OSc(CH_4)$ complex, which was predicted to have a C_{3v} symmetry analogous to the $OTi(CH_4)$ complex with a predicted binding energy of 1.2 kcal/mol at the CCSD(T)//B3LYP level. No further reaction was observed from $OSc(CH_4)$. For CrO, CoO and NiO, no reaction was observed. Recent studies in our laboratory have shown that some transition metal oxide molecules trapped in solid argon are chemically coordinated by one or multiple argon atoms in forming the noble gas complexes.[96–99] The late transition metal monoxides (CrO through NiO) trapped in solid argon were found to be coordinated by one argon atom with quite strong metal–Ar binding energies.[99] If the binding energy of Ar is stronger than that of methane, the reaction of metal monoxide with methane will be blocked due to Ar coordination.

3.4. *Periodic trends*

The initial step for the reactions of transition metal monoxides with methane is the formation of the 1:1 $OM(CH_4)$ complex. The $OSc(CH_4)$, $OTi(CH_4)$, $ONb(CH_4)$, $OFe(CH_4)$ and $OMn(CH_4)$ complexes were experimentally observed. The $OSc(CH_4)$ and $OTi(CH_4)$ complexes were predicted to have a C_{3v} symmetry with one H atom of CH_4 coordinated to the O atom, whereas the other complexes have C_{2v} or C_{3v} symmetry with the metal atom coordinated to two or three hydrogen atoms of the methane molecule. While the interaction between transition metal monoxide and methane is very weak, the late transition metal monoxides bound more strongly than that of early transition metal monoxides. The CH_4 molecule is spherical and is difficult to be polarized. It is a very poor ligand that may be comparable to the argon atom. The ScO and TiO molecules are more ionic than late transition metal monoxides; the bonding between ScO or TiO and methane is largely ion induced dipole interaction. The late transition metal monoxides have quite low metal based valence molecular orbitals, which are responsible for bonding interactions with methane, as have been discussed in late transition metal–noble gas complexes.[99]

Different oxidation reaction mechanisms were observed starting from the $OM(CH_4)$ complexes, as illustrated in Scheme 3.

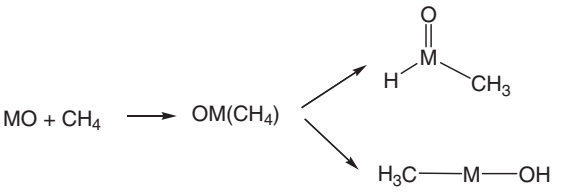

Scheme 3. The mechanisms for the $MO + CH_4$ reactions.

Table 1. Bond dissociation energies (BDE, in eV) for the MO molecules. From ref. 100.

	State	BDE
TiO	$^3\Delta$	6.87
NbO	$^4\sum^-$	7.53
TaO	$^2\Delta$	8.2
MnO	$^6\sum^+$	3.83
FeO	$^5\Delta$	4.17

From the complex, one hydrogen atom of methane is transferred to the metal centre to form the $CH_3M(O)H$ structure for the early transition metals (Ti, Nb, Ta).[86,87] In contrast, the hydrogen atom of methane is transferred to the O atom to give the CH_3MOH isomer for the late transition metals (Mn, Fe).[85] The different reactivity can be rationalized in terms of changes in the strength of the M–O bonds and the electron count. As listed in Table 1, the bond dissociation energies of early transition metal monoxides are significantly larger than those of late transition metal monoxides.[100] Among the oxides studied, the NbO and TaO molecules have bond dissociation energies above 7.5 eV, about twice as large as those of MnO and FeO. Therefore, the hydrogen atom prefers to be transferred to the O atom for late transition metals, whereas the hydrogen atom is firstly added to the metal centre for early transition metals. The bond dissociation energy of TiO is significantly higher than those of MnO and FeO, but is lower than those of NbO and TaO. Therefore, after the first hydrogen atom transfer to the Ti centre in forming the $CH_3Ti(O)H$ intermediate, a second hydrogen atom is able to be transferred subsequently to the O atom in forming the $CH_2Ti(H)OH$ isomer in the $TiO + CH_4$ reaction. For the addition of the C–H bond to the M=O bond in forming the CH_3MOH structure, the valence of metal remains in its +2 oxidation state, but if the C–H bond adds to the metal atom to form the $CH_3M(O)H$ isomer, the oxidation state of metal increases from +2 to +4. The valence d electrons of early transition metals are inclined to participate in bonding to form high-valent compounds, whereas the late transition metals, Mn and Fe, prefer to form divalent molecules due to the stability of the half and more than half filled d^5 and d^6 electronic configurations. A similar difference in reactivity between early and late transition metals has previously been reported for some other reactants such as H_2O[101–106] and NH_3.[107–111]

4. The M + CH_3OH reactions

There are some reports on matrix isolation spectroscopic study on the reactions of neutral metal atoms with methanol, which showed that the reactivity of methanol toward metal atoms is diverse and heavily depends on the metals.[112–118] Earlier studies of iron atom reaction with methanol have identified the formation of the Fe(CH_3OH) complex. Subsequent photoexcitation of the complex in the visible region ($\lambda > 400$ nm) led to iron insertion into the O–H bond, whereas UV (280 nm $< \lambda <$ 360 nm) irradiation caused the activation of the C–O bond.[112] Silicon atoms inserted into both the O–H and C–O bonds of methanol to form methoxysilylene and methylsilicon hydroxide in solid argon, but the O–H bond insertion is energetically favoured over the C–O bond insertion.[113,114] The reactions of laser-ablated boron atoms with methanol produced CH_3BO as well as CH_2BOH and CH_2BO, which were formed *via* boron insertion into the C–O bond of methanol.[115] Recent investigations in our laboratory on the reactions of beryllium and magnesium atoms with methanol in solid argon have shown that the ground state beryllium atoms spontaneously inserted into the O–H bond of methanol to form CH_3OBeH; the thermodynamically more favourable CH_3BeOH and CH_3MgOH were only formed upon broad-band irradiation.[116,117] In contrast, no electron paramagnetic resonance evidence was found for aluminium atom insertion into the C–O, C–H and O–H bonds of methanol in an adamantine matrix at 77 K.[118] Being considered as the reverse reaction of MO + CH_4, complementary investigations were performed on the reactions of the first row transition metal atoms and methanol.

4.1. *Sc + CH_3OH*

The ground state Sc atoms react with methanol to form the inserted CH_3OScH molecule spontaneously on annealing in solid argon, as clearly shown in Figure 7.[119] The CH_3OScH molecule was predicted to have a $^2A'$ ground state with a C_s symmetry. Under broad-band UV light irradiation, CH_3OScH isomerizes to the OSc(CH_4) complex or decomposes to ScO and CH_4.

4.2. *Ti + CH_3OH*

Ti atoms are reactive toward methanol,[87,120] and form complexes with methanol bound by 12.4 kcal/mol without a barrier. Under visible light irradiation, the dominant reaction channel is an insertion into the O–H bond of methanol to produce the CH_3OTiH molecule. The CH_3OTiH intermediate further rearranges to the $CH_3Ti(O)H$ and $CH_2Ti(H)OH$ isomers upon UV light excitation, which are also observed in the TiO + CH_4 reaction.[87]

4.3. *Mn, Fe + CH_3OH*

The reactions of late transition metal atoms with methanol in a solid matrix have been studied by Margrave and coworkers.[112] The experimental observations show that the ground state metal atoms react with methanol to form stable molecular

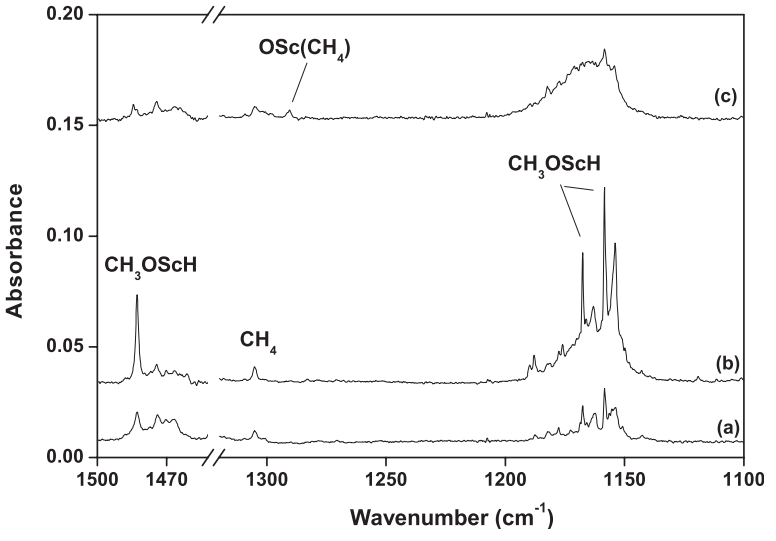

Figure 7. Infrared spectra in selected regions from co-deposition of laser-evaporated scandium atoms with 0.2% CH_3OH in argon. (a) 1 h of sample deposition at 12 K; (b) after 24 K annealing; and (c) after 30 min of broad-band ($250 < \lambda < 580$ nm) irradiation.

complexes. Photoexcitation of the complexes in the visible region ($\lambda > 400$ nm) led to metal insertion into the O–H bond of methanol in forming the CH_3OMH molecules, whereas UV ($280\text{ nm} < \lambda < 360$ nm) irradiation caused the activation of the C–O bond of methanol in forming the CH_3MOH, which were also observed in the $MO + CH_4$ reactions. The CH_3FeOH structure was predicted to be 28.3 kcal/mol lower in energy than the CH_3OFeH isomer at the B3LYP level.[120]

In the experiments with relatively high metal atom concentrations, the CH_3MOH or CH_3OMH intermediates are able to react with a second metal atom to form the dinuclear CH_3MOMH molecules upon UV ($\lambda > 300$ nm) light irradiation. The reaction mechanism is similar to that of $M + H_2O$.[104–106] For the latter, the MOH_2 complexes were formed, and the metal inserts into one of the O–H bonds of water to give the HMOH molecule, which further reacts with a second metal atom to form HMOMH.[104–106]

4.4. *Mechanisms of methane-to-methanol conversion*

Based on the experimentally probed intermediates in both the $MO + CH_4$ and $M+CH_3OH$ reactions, some information regarding the mechanism of methane-to-methanol conversion by transition metal monoxides can be drawn. For late transition metals Mn and Fe, the inserted CH_3MOH molecule is a critical intermediate observed in both the $MO + CH_4$ and $M+CH_3OH$ reactions. The major reaction pathway involved is assumed as follows:

$$MO + CH_4 \rightarrow OM(CH_4) \rightarrow CH_3MOH \rightarrow M(CH_3OH) \rightarrow M + CH_3OH.$$

In this view, the mechanism of the neutral reaction is similar to that of the methane-to-methanol conversion by late transition metal monoxide cations.[21,30,36] The potential

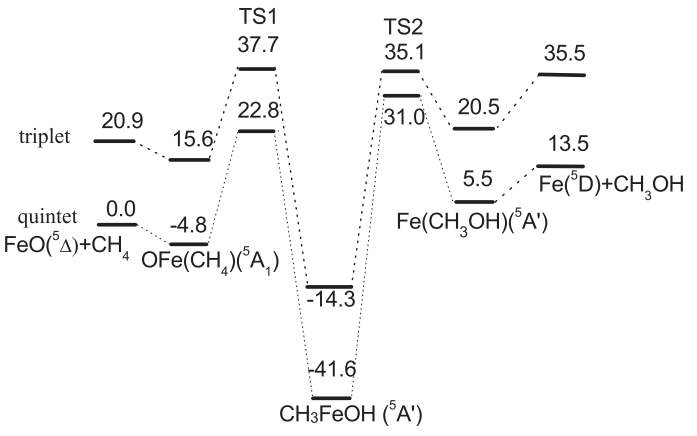

Figure 8. The potential energy profiles of the $FeO + CH_4 \rightarrow Fe + CH_3OH$ reaction calculated at the B3LYP/6-311++G** level. From ref. 85.

energy surfaces along the $MO + CH_4 \rightarrow CH_3OH + M$ (M = Mn, Fe) reaction path have been computed at the B3LYP/6-311++G** level, and the results for iron are shown in Figure 8. The reaction follows a mechanism similar to that of the $FeO^+ + CH_4 \rightarrow Fe^+ + CH_3OH$ reaction. However, the FeO neutral reaction proceeds only on the quintet surface, and no spin crossing was observed, which is different from the FeO^+ cation reaction, in which crossings between the high-spin and low-spin potential energy surfaces were predicted to occur. The potential energy surface shown in Figure 8 indicates that the initial reaction step is the attachment of methane to the Fe centre of FeO to form the $OFe(CH_4)$ complex without any barrier. From the complex, the reaction proceeds by a hydrogen atom migration from C to O *via* a transition state (TS1) to form the CH_3FeOH intermediate. The barrier height from the $OFe(CH_4)$ complex to the CH_3FeOH structure is about 27.6 kcal/mol, which is in accord with the experimental observation that CH_3FeOH was only produced upon UV light irradiation. From the CH_3FeOH intermediate, the reaction proceeds to $Fe(CH_3OH)$ by the methyl group migration *via* the transition state TS2. This reaction step is highly endothermic by 47.1 kcal/mol. The barrier for the methyl group migration at TS2 is as high as 72.6 kcal/mol. The $Fe(CH_3OH)$ complex decomposes to $Fe + CH_3OH$ without a barrier. Overall, the $FeO + CH_4 \rightarrow Fe + CH_3OH$ reaction was predicted to be endothermic by 13.5 kcal/mol, and proceeds *via* two transition states, which lie 22.8 and 35.1 kcal/mol above the ground state reactants. We were not able to observe the formation of $Fe(CH_3OH)$ from CH_3FeOH because of the significant barrier at TS2.

The reaction mechanism for early transition metals is different from that of late transition metals. The CH_3MOH intermediate was observed neither in the $MO + CH_4$ reaction nor in the $M + CH_3OH$ reaction. In contrast, the $CH_3M(O)H$ molecule was observed to be an important intermediate in both the $MO + CH_4$ and $M + CH_3OH$ reactions for group IV and V transition metals. The CH_3OMH structure is determined to be an intermediate in the reaction pathway from the $M(CH_3OH)$ complex to the

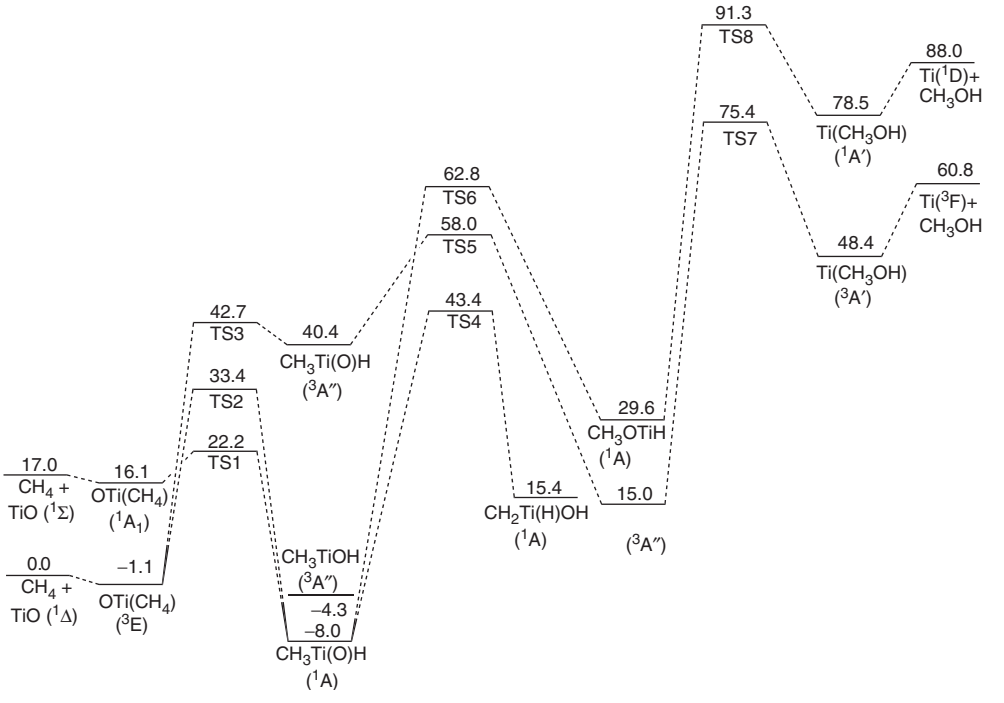

Figure 9. Potential energy profiles for the $TiO + CH_4 \rightarrow Ti + CH_3OH$ reaction calculated at the CCSD(T)/6-311++G**/B3LYP/6-311++G (3df, 3pd) level of theory (values are given in kcal/mol).

$CH_3M(O)H$ structure. Therefore, the reaction pathway from methane to methanol is proposed as:

$$MO + CH_4 \rightarrow OM(CH_4) \rightarrow CH_3M(O)H \rightarrow CH_3OMH \rightarrow M(CH_3OH) \rightarrow M + CH_3OH.$$

The potential energy profiles for the $TiO + CH_4$ reaction calculated at the CCSD(T)/6-311++G**/B3LYP/6-311++G (3df, 3pd) level of theory are shown in Figure 9. The initial interaction between the $^3\Delta$ ground state TiO and methane is the formation of the 1:1 complex without any barrier. From the complex, the reaction proceeds by hydrogen atom migration from C to the metal centre to form the $CH_3Ti(O)H$ intermediate. Since the $OTi(CH_4)$ has a triplet (^3E) ground state, while the $CH_3Ti(O)H$ molecule has a singlet ground state, there is a spin crossing between the triplet and singlet potential energy surfaces. This reaction step is exothermic by 6.9 kcal/mol with a barrier of 23.3 kcal/mol (TS1). Since the CH_3MOH structure is the critial intermediate involved in the late transition metal monoxide reactions, we also calculated the reaction path from $OTi(CH_4)$ to CH_3TiOH. This process proceeds by a hydrogen atom migration from C to O *via* a transition state (TS2) lying 11.2 kcal/mol above TS1. The CH_3TiOH structure was predicted to be 3.7 kcal/mol higher in energy than the $CH_3Ti(O)H$ isomer. Therefore, the formation of CH_3TiOH is energetically unfavoured and is not observed experimentally. From the $CH_3Ti(O)H$ intermediate, the reaction proceeds to the CH_3OTiH intermediate by the methyl group migration. The CH_3OTiH intermediate has a $^3A''$ ground state, which

lies about 23.0 kcal/mol above the singlet $CH_3Ti(O)H$ isomer. There is another spin crossing from $CH_3Ti(O)H$ to CH_3OTiH. The energy barrier (TS5) for this process is 66.0 kcal/mol with respect to $CH_3Ti(O)H$. From the CH_3OTiH intermediate, the reaction proceeds to $Ti(CH_3OH)$ *via* transition state TS7. This reaction step is highly endothermic by 33.4 kcal/mol with a barrier as high as 60.4 kcal/mol. The $Ti(CH_3OH)$ complex decomposes to $Ti + CH_3OH$ without a barrier. Overall, the $TiO + CH_4 \rightarrow Ti + CH_3OH$ reaction was predicted to be endothermic by 60.8 kcal/mol, and spin crossing occurs twice along the entire reaction pathway. There is another reaction pathway from $CH_3Ti(O)H$, that is, one hydrogen atom of CH_3 group can further be transferred to the O atom in $CH_3Ti(O)H$ to form the $CH_2Ti(H)OH$ isomer. This process is slightly endothermic (23.4 kcal/mol) and proceeds *via* a transition state (TS4) lying 51.4 kcal/mol above $CH_3Ti(O)H$. Note that TS4 lies 14.6 kcal/mol below TS5, thus, the isomerization to $CH_2Ti(H)OH$ should be energetically favourable compared to the reaction pathway toward the CH_3OTiH intermediate. Consistent with the above notion, the $CH_2Ti(H)OH$ molecule instead of the CH_3OTiH isomer was formed in the $TiO + CH_4$ experiments.

In the case of scandium, the reaction mechanism is different from that of the group IV and V metals. Although no intermediate except the $OSc(CH_4)$ complex was observed in the $ScO + CH_4$ reaction, the CH_3OScH molecule was observed to be an intermediate in the $Sc + CH_3OH$ reaction. Therefore, the reverse reaction pathway can be described as:

$$Sc + CH_3OH \rightarrow CH_3OScH \rightarrow OSc(CH_4) \rightarrow ScO + CH_4.$$

The potential energy surface for the reaction of ScO with methane has been calculated by Mebel and coworkers at the DFT/B3LYP level.[82,83] Their calculations show that scandium monoxide is unable to form a stable molecular complex with methane, instead, the reaction proceeds by insertion of ScO into the C–H bond to form the CH_3ScOH intermediate *via* a transition state. They did not consider the CH_3OScH intermediate. The potential energy profile on the doublet surface of the $ScO + CH_4 \leftrightarrow Sc + CH_3OH$ reaction calculated at the B3LYP/6-311++G(d,p) level is illustrated in Figure 10. The initial step of the $ScO + CH_4$ reaction is the formation of a very weakly bound $OSc(CH_4)$ complex. From the complex, two reaction paths are considered. The first path is hydrogen atom migration to the Sc centre to form the $CH_3Sc(O)H$ intermediate *via* a transition state (TS1); the $CH_3Sc(O)H$ intermediate subsequently isomerizes to the CH_3OScH structure *via* the methyl group migration, which further rearranges to the $Sc(CH_3OH)$ complex *via* transition state TS5. The second path is one hydrogen atom migration from C to the O atom to form the CH_3ScOH intermediate *via* a transition state (TS2). The CH_3ScOH intermediate dissociates to form $CH_3 + ScOH$ without energy barrier. The $CH_3 + ScOH$ products recombine to form the $Sc(CH_3OH)$ complex *via* a transition state (TS4). The second path is about the same as that reported by Mebel and coworkers.[82,83] According to our calculations, the CH_3ScOH molecule is 19.8 kcal/mol more stable than the CH_3OScH isomer. The transition states involved in the reaction path from $ScO + CH_4$ to CH_3OScH lie considerably high compared to that of the reaction path from $ScO + CH_4$ to CH_3ScOH. Thus, the second path leading to the CH_3ScOH intermediate should be energetically favourable compared to the first path with the formation of CH_3OScH. In contrast, the transition state involved in the reaction path from CH_3ScOH to

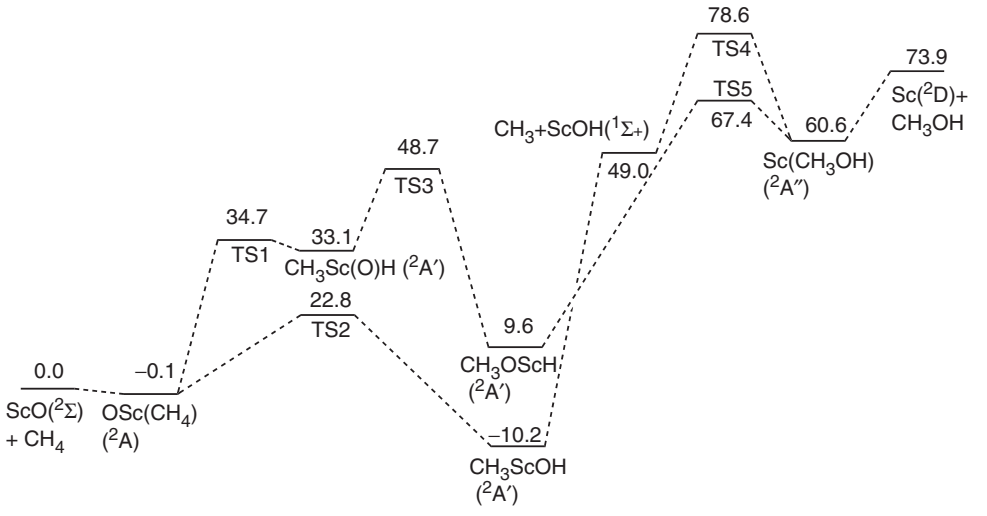

Figure 10. Potential energy profiles for the $ScO + CH_4 \rightarrow Sc + CH_3OH$ reaction calculated at the B3LYP/6-311++G** level of theory (values are given in kcal/mol).

$Sc(CH_3OH)$ lies above that of the second path from CH_3OScH to $Sc(CH_3OH)$. Therefore, the ground state Sc atom reacted with methanol to form CH_3OScH, but not the thermodynamically more favourable CH_3ScOH.

The above proposed reaction pathways for early transition metal reaction systems are quite different from that previously reported for transition metal monoxide cation reactions. The corresponding $[CH_3OMH]^+$ and/or $[CH_3M(O)H]^+$ intermediates have not been considered in previous investigations on the cation systems. We assume that such species may also be important intermediates in the reactions of early transition metal monoxide cations.

Similar to cation reactions, the reaction pathway from methane to methanol is quite uphill in energy on early transition metal monoxides according to theoretical calculations, which suggest that early transition metal monoxides are not good mediators for the formation of methanol. In contrast, the late transition metal monoxides are expected to be more efficient in converting methane to methanol, as the reaction from methane to methanol is almost thermally neutral or slightly uphill for late transition metal monoxides.

5. The vibrational frequencies of the intermediates

As has been discussed above, the intermediates involved in the $MO + CH_4$ and $M + CH_3OH$ reactions were trapped in solid argon, and their infrared vibrational spectra were measured. The stoichiometry and vibrational modes of the observed intermediates were determined based on the isotopic substitutions, and the assignments were further supported by density functional theoretical frequency calculations. Density functional calculations with sophisticated functionals and basis sets generally provide quite reliable predictions on the vibrational frequencies and intensities for ground state transition metal-containing compounds. The deviations obtained at the B3LYP level usually amount to

several percent. The anharmonicity and matrix shift are expected to be the major contributors to these deviations. In addition, the calculated isotopic frequency shifts or ratios, which are characteristic of the nature for normal mode of vibrations, provide additional key factors to be compared with experiment. None of these intermediates have been spectroscopically characterized in the gas phase. The vibrational frequencies of such neutral species in solid argon are expected to be slightly shifted from the gas phase values, and they provide a significantly good approximation to the gas phase band centres.

5.1. *OM(CH_4)*

The vibrational frequencies of the M–O stretching and CH_2 deformation modes of the OM(CH_4) complexes in solid argon are listed in Table 2. The frequency shifts with respect to the free MO and CH_4 molecules in solid argon are also listed. Upon complex formation, the structure of the methane unit is deformed from the T_d-type geometry of free methane into a low symmetry structure. Thus, the IR active triply degenerate CH_2 deformation mode splits into two or more IR active modes due to reduced symmetry, and the frequencies are shifted from that of free methane. However, if the shift is not large enough, it will be overlapped by the strong free methane absorption. Only one CH_2 deformation mode was observed for most of the systems studied. For early transition metals, both the M–O stretching and CH_2 deformation modes are red-shifted with respect to free MO and methane in solid argon. In contrast, both modes are blue-shifted for the late transition metals. It should be mentioned that the late transition metal monoxides (MnO and FeO) are coordinated by one Ar atom in solid argon, therefore, the shifts of the M–O stretching mode listed in Table 2 should be regarded as the difference between OM(CH_4) and OM(Ar).

5.2. *CH_3MOH*

The CH_3MOH intermediates were observed only in the late transition metal systems. Only two vibrational modes were observed for the CH_3FeOH molecule, namely, the M–OH stretching and O–H stretching modes observed at 687.5 and 3744.8 cm^{-1} in solid argon.

Table 2. Vibrational frequencies (cm^{-1}) of the M–O stretching and CH_2 deformation modes of OM(CH_4) and frequency shifts (cm^{-1}) with respect to free MO and CH_4.

	M–O stretch		CH_2 deformation	
	ν	$\Delta\nu$[a]	ν	$\Delta\nu$
OSc(CH_4)	944.2	−2.8	1290.2	−15.2
OTi(CH_4)	974.1	−13.9	1285.8	−19.6
ONb(CH_4)	947.1	−16.8	1289.8	−15.6
OMn(CH_4)	842.1	8.8		
OFe(CH_4)	879.4	6.6	1355.2, 1323.3	49.8
				17.9

Note: [a]Three site absorptions were observed for TiO in solid argon;[122] the average value is used.

The corresponding absorptions for the deuterium substituted species are shifted to 667.2 and 2759.8 cm^{-1}. Only the Mn–OH stretching mode was observed at 661.4 cm^{-1} for the CH_3MnOH intermediate.

5.3. *CH_3OMH*

The CH_3OMH intermediates were formed either from spontaneous reaction of atomic Sc with methanol or from electronically exciting the metal–methanol complexes. The vibrational frequencies for the first row transition metals, Sc through Fe, are given in Table 3. For all of the CH_3OMH intermediates, the M–H and C–O stretching modes are the strongest absorptions in the infrared spectra. As can be seen in Table 3, while the C–O stretching modes were observed around 1150 cm^{-1} for all of the CH_3OMH molecules, the M–H stretching frequencies increase across the series from 1482.7 cm^{-1} in CH_3OScH to 1767.0 cm^{-1} in CH_3OFeH. The increase of the M–H stretching frequency is largely due to the regular reduction in metal ionic radius with increasing atomic number across the series. A similar trend has also been observed for the M–H stretching modes of the HMOH molecules in the reactions of first row transition metal atoms with water.[42]

5.4. *$CH_3M(O)H$*

The $CH_3M(O)H$ intermediates were formed only for early transition metal systems, including group IV and V metals. The experimentally observed vibrational frequencies are listed in Table 4. These intermediates are characterized as having two strong IR active vibrations, the terminal M–H and M=O stretching vibrations.

5.5. *$M(CH_3OH)$*

The $M(CH_3OH)$ complexes were obtained for all of the $M + CH_3OH$ reactions studied except Sc. The ground state Sc atoms was found to react with methanol to form the inserted CH_3OScH intermediate spontaneously, which suggests that $Sc(CH_3OH)$ is a short-lived species, and is not able to be stabilized in solid argon matrix. Sc is a very electropositive element, and the $Sc + CH_3OH$ reaction to form CH_3OScH is highly

Table 3. Vibrational frequencies (cm^{-1}) of the CH_3OMH intermediates in solid argon.

	Frequency						
	CH_3 asym stretch	CH_3 sym stretch	M–H stretch	CH_3 bend	C–O stretch	M–OCH_3 stretch	M–H bend
CH_3OScH			1482.7	1167.4	1158.5	562.2	
CH_3OTiH			1520.4		1149.9		
CH_3OVH			1567.1		1150.5		
CH_3OCrH	2885.6	2818.3	1662.1	1165.0	1139.5	552.8	477.0
CH_3OMnH		2819.6	1694.3		1156.6	529.2	
CH_3OFeH			1767.0		1155.9		

Table 4. Vibrational frequencies (cm^{-1}) of the $CH_3M(O)H$ intermediates in solid argon.

	Frequency				
	M–H stretch	CH_3 bend	M=O stretch	M–CH_3 stretch	M–H bend
$CH_3Ti(O)H$	1613.9		1000.4	583.7	474.7
$CH_3Zr(O)H$	1542.9		914.7		
$CH_3Nb(O)H$	1686.6		973.4		
$CH_3Ta(O)H$	1766.6	1160.8	974.7		

Table 5. Vibrational frequencies (cm^{-1}) of the $M(CH_3OH)$ complexes in solid argon.

	Frequency		
	O–H stretch	CH_3 bend	C–O stretch
$Ti(CH_3OH)$		1063.2	968.7
$V(CH_3OH)$			974.4
$Cr(CH_3OH)$	3627.4		1008.3
$Mn(CH_3OH)$	3613.7	1060.8	994.0
$Fe(CH_3OH)$			987.6

exothermic. The $M(CH_3OH)$ complexes are more strongly bound than the $OM(CH_4)$ complexes. The vibrational frequencies of the experimentally observed $M(CH_3OH)$ complexes are summarized in Table 5. The C–O stretching mode is the most IR intense absorption for all of the complexes, which is red-shifted with respective to free methanol. Methanol is a ligand that is similar to water. Although methanol cannot act as a π acceptor, it is an electron donor. The metal is coordinated with the O atom of methanol. The donation of electron density from the lone pair orbital of methanol to metal weakens the C–O bond, which results in a decrease of the C–O stretching frequency.

6. Conclusions

We have shown in this article some of our recent studies in probing the reaction intermediates involved in the methane-to-methanol conversion process by the neutral transition metal monoxides. Important intermediates in both the $MO + CH_4$ and $M + CH_3OH$ reactions (M = transition metals) were trapped and detected by matrix isolation infrared absorption spectroscopy. The vibrational frequencies of intermediates isolated in solid argon were measured and assigned on the basis of isotopic substitutions. Complementary quantum chemical calculations were performed to validate the experimental assignments and to gain a detailed understanding of the reaction mechanism. This involves calculations not only of the equilibrium geometries and vibrational spectra of the intermediates experimentally detected, but also energetics and potential energy surfaces of the reactions.

For late transition metals, the inserted CH_3MOH molecule is a critical intermediate in the reactions. The major reaction pathway involved is as follows:

$$MO + CH_4 \rightarrow OM(CH_4) \rightarrow CH_3MOH \rightarrow M(CH_3OH) \rightarrow M + CH_3OH$$

which is similar to that of the methane-to-methanol conversion by transition metal monoxide cations. However, the cation system is characterized as involving two-state reactivity, while the reactions of late transition metal neutrals proceed on a single potential energy surface.

Different oxidation reaction mechanisms were observed for early transition metal systems. The inserted CH_3OMH and $CH_3M(O)H$ molecules are critical intermediates in group IV and V transition metals, and the reaction pathway is proposed as:

$$MO + CH_4 \rightarrow OM(CH_4) \rightarrow CH_3M(O)H \rightarrow CH_3OMH \rightarrow M(CH_3OH) \rightarrow M + CH_3OH.$$

For Sc, the CH_3ScOH molecule is an important intermediate involved in the $ScO + CH_4$ reaction, whereas, the CH_3OScH is a critical intermediate involved in the $Sc + CH_3OH$ reaction.

The proposed reaction pathways for early transition metal reaction systems are quite different from that previously reported for transition metal monoxide cation reactions. We assume that the analogous $[CH_3OMH]^+$ and/or $[CH_3M(O)H]^+$ species may also be important intermediates in the reactions of early transition metal monoxide cations, which have never been considered.

These investigations clearly demonstrate that matrix isolation spectroscopy coupled with quantum chemical calculations is a powerful method for delineating reaction mechanisms by facilitating the isolation and characterization of the reactive intermediates.

The systems we have studied to date are the simplest model systems concerning catalytic methane-to-methanol conversion. We hope to extend our studies to larger systems such as metal oxide clusters, which should be more perfect models for the catalyst surface and active site of enzyme. The major difficulty is how to produce and trap metal oxide clusters into solid matrix with detectable concentrations. The reactivity of metal oxides in different oxidation states and in different media is also of fundamental interest. Besides matrix isolation infrared spectroscopic technique, it will be very helpful to investigate these more complicated systems using other complementary techniques.

Acknowledgements

Financial support from the National Basic Research Program of China (Grant No. 2004CB719501 and 2007CB815203) and the National Natural Science Foundation of China (Grant No. 20125311 and 20433080) is gratefully acknowledged. The studies outlined in this review are the work of group members: Dr. Mohua Chen, and graduate students Zhenguo Huang and Yu Gong.

References

[1]H.D. Gesser, N.R. Hunter and C.B. Prakash, Chem. Rev. **85**, 235 (1988).
[2]R.H. Crabtree, Chem. Rev. **95**, 987 (1995).
[3]A.E. Shilov and G.B. Shul'pin, Chem. Rev. **97**, 2879 (1997).
[4]J. Haggin, Chem. Eng. News **71**, 27 (1993).

[5]S.H. Taylor, J.S.J. Hargreaves, G.J. Hutchings and R.W. Joyner, Appl. Catal. A **126**, 287 (1995).
[6]S.H. Taylor, J.S.J. Hargreaves, G.J. Hutchings, R.W. Joyner and C.W. Lembacher, Catal. Today **42**, 217 (1998).
[7]M. Baerns and O. Buyevskaya, Catal. Today **45**, 13 (1998).
[8]R.A. Periana, D.J. Taube, E.R. Evitt, D.G. Löffler, P.R. Wentrcek, G. Voss and T. Masuda, Science **259**, 340 (1993).
[9]R.A. Periana, D.J. Taube, T.S. Gamble, H. Taube, T. Satoh and H. Fujii, Science **280**, 560 (1998).
[10]M.H. Baik, M. Newcomb, R.A. Friesner and S.J. Lippard, Chem. Rev. **103**, 2385 (2003).
[11]T.C. Jackson, D.B. Jacobson and B.S. Freiser, J. Am. Chem. Soc. **106**, 1252 (1984).
[12]T.C. Jackson, T.J. Cadin and B.S. Freiser, J. Am. Chem. Soc. **108**, 1120 (1986).
[13]H. Kang and J.L. Beauchamp, J. Am. Chem. Soc. **108**, 1502 (1986).
[14]K.K. Irikura and J.L. Beauchamp, J. Am. Chem. Soc. **111**, 75 (1989).
[15]C.J. Cassady and S.W. McEhrany, Organometallics **11**, 2367 (1992).
[16]D. Schroder and H. Schwarz, Angew. Chem. Int. Ed. Engl. **29**, 1433 (1990).
[17]H. Schwarz, Angew. Chem. Int. Ed. Engl. **30**, 820 (1991).
[18]Y.M. Chen, D.E. Clemmer and P.B. Armentrout, J. Am. Chem. Soc. **116**, 7815 (1994).
[19]M.F. Ryan, A. Fiedler, D. Schroder and H. Schwarz, Organometallics **13**, 4072 (1994).
[20]M.F. Ryan, A. Fiedler, D. Schroder and H. Schwarz, J. Am. Chem. Soc. **117**, 2033 (1995).
[21]D. Schröder and H. Schwarz, Angew. Chem. Int. Ed. Engl. **34**, 1973 (1995).
[22]D. Schroder, H. Schwarz, D.E. Clemmer, Y.M. Chen, P.B. Armentrout, V.I. Baranov and D. K. Bohme, Int. J. Mass Spectrom. Ion Processes **161**, 175 (1997).
[23]J.N. Harveya, M. Diefenbach, D. Schroder and H. Schwarz, Int. J. Mass Spectrom. Ion Processes **182/183**, 85 (1999).
[24]A. Fiedler, D. Schroder, S. Shaik and H. Schwarz, J. Am. Chem. Soc. **116**, 10734 (1994).
[25]K. Yoshizawa, Y. Shiota and T. Yamabe, Chem. Eur. J. **3**, 1160 (1997).
[26]K. Yoshizawa, Y. Shiota and T. Yamabe, J. Am. Chem. Soc. **120**, 564 (1998).
[27]K. Yoshizawa, Y. Shiota and T. Yamabe, Organometallics **17**, 2825 (1998).
[28]K. Yoshizawa, Y. Shiota and T. Yamabe, J. Chem. Phys. **111**, 538 (1999).
[29]K. Yoshizawa, Y. Shiota, Y. Kagawa and T. Yamabe, J. Phys. Chem. A **104**, 2552 (2000).
[30]Y. Shiota and K. Yoshizawa, J. Am. Chem. Soc. **122**, 12317 (2000).
[31]Y. Shiota and K. Yoshizawa, J. Chem. Phys. **118**, 5872 (2003).
[32]G.B. Zhang, S.H. Li and Y.S. Jiang, Organometallics **23**, 3656 (2004).
[33]M. Azzaro, S. Breton, M. Decouzon and S. Geribaldi, Int. J. Mass Spectrom. Ion Processes **1**, 128 (1993).
[34]D. Schroder, A. Fiedler, J. Hrusik and H. Schwarz, J. Am. Chem. Soc. **114**, 1215 (1992).
[35]F. Aguirre, J. Husband, C.J. Thompson, K.L. Stringer and R.B. Metz, J. Chem. Phys. **116**, 4071 (2002).
[36]R.B. Metz, Int. Rev. Phys. Chem. **23**, 79 (2004).
[37]J.C. Weisshaar, Acc. Chem. Res. **26**, 213 (1993).
[38]M.J. Pilling and P.W. Seakins, *Reaction Kinetics* (Oxford University Press, Oxford, 1995).
[39]V.E. Bondybey, A.M. Smith and J. Agreiter, Chem. Rev. **96**, 2113 (1996).
[40]M.F. Zhou, L. Andrews and C.W. Bauschlicher Jr, Chem. Rev. **101**, 1931 (2001).
[41]H.J. Himmel, A.J. Downs and T.M. Greene, Chem. Rev. **102**, 4191 (2002).
[42]L. Andrews and M. Moskovits, *Chemistry and Physics of Matrix Isolated Species* (North Holland, Amsterdam, 1989).
[43]M.E. Jacox, Acc. Chem. Res. **37**, 727 (2004).
[44]L. Andrews and H.G. Cho, Organometallics **25**, 4040 (2006).
[45]W.E. Billups, M.M. Konarski, R.H. Hauge and J.L. Margrave, J. Am. Chem. Soc. **102**, 7393 (1980).
[46]G.A. Ozin, D.F. McIntosh and S.A. Mitchell, J. Am. Chem. Soc. **103**, 1574 (1981).

[47]S.C. Chang, R.H. Hauge, W.E. Billups, Z.H. Kafafi and J.L. Margrave, Inorg. Chem. **27**, 205 (1988).
[48]P. Hassanzadeh and L. Andrews, J. Am. Chem. Soc. **114**, 9239 (1992).
[49]P. Harrcranzadeh, Y. Hamachi and L. Andrews, J. Phys. Chem. **97**, 6418 (1993).
[50]T.M. Greene, L. Andrews and A.J. Downs, J. Am. Chem. Soc. **117**, 8180 (1995).
[51]T.M. Greene, D.V. Lanzissera, L. Andrews and A.J. Downs, J. Am. Chem. Soc. **120**, 6097 (1998).
[52]H.J. Himmel, A.J. Downs, T.M. Greene and L. Andrews, Organometallics **19**, 1060 (2000).
[53]G. Maier, H.P. Reisenauer and J. Glatthaar, Chem. Eur. J. **8**, 4383 (2002).
[54]A. Bihlmeier, T.M. Greene and H.J. Himmel, Organometallics **23**, 2350 (2004).
[55]H.J. Himmel, Chem. Eur. J. **10**, 2851 (2004).
[56]G.J. Wang, M.H. Chen and M.F. Zhou, Chem. Phys. Lett. **412**, 46 (2005).
[57]L. Andrews, H.G. Cho and X.F. Wang, Inorg. Chem. **44**, 4834 (2005).
[58]L. Andrews, H.G. Cho and X.F. Wang, Angew. Chem. Int. Ed. **44**, 113 (2005).
[59]L. Andrews, H.G. Cho and X.F. Wang, J. Am. Chem. Soc. **127**, 465 (2005).
[60]H.G. Cho, X.F. Wang and L. Andrews, Organometallics **24**, 2854 (2005).
[61]H.G. Cho and L. Andrews, J. Am. Chem. Soc. **127**, 8226 (2005).
[62]H.G. Cho, L. Andrews and C. Marsden, Inorg. Chem. **44**, 7634 (2005).
[63]L. Andrews and H.G. Cho, J. Phys. Chem. A. **109**, 6796 (2005).
[64]H.G. Cho, L. Andrews and C. Marsden, Inorg. Chem. **44**, 7634 (2005).
[65]H.G. Cho and L. Andrews, J. Am. Chem. Soc. **127**, 8226 (2005).
[66]H.G. Cho and L. Andrews, J. Phys. Chem. A **110**, 3886 (2006).
[67]H.G. Cho and L. Andrews, Organometallics **26**, 633 (2007).
[68]V.E. Bondybey, J. Phys. Chem. **86**, 3396 (1982).
[69]T.R. Burkholder and L. Andrews, J. Chem. Phys. **95**, 8697 (1991).
[70]M.H. Chen, X.F. Wang, L.N. Zhang, M. Yu and Q.Z. Qin, Chem. Phys. **242**, 81 (1999).
[71]C.W. Bauschlicher Jr, A. Ricca, H. Partridge and S.R. Langhoff, in *Recent Advances in Density Functional Theory*, Part II. edited by D.P. Chong (World Scientific Publishing, Singapore, 1997).
[72]I. Bytheway and M.W. Wong, Chem. Phys. Lett. **282**, 219 (1998).
[73]P.E.M. Siegbahn, *Electronic Structure Calculations for Molecules Containing Transition Metals,* Adv. Chem. Phys. **XCIII**, 333 (1996).
[74]M.J. Frisch, G.W. Trucks, H.B. Schlegel, G.E. Scuseria, M.A. Robb, J.R. Cheeseman, J.A. Montgomery, Jr., T. Vreven, K.N. Kudin, J.C. Burant, J.M. Millam, S.S. Iyengar, J. Tomasi, V. Barone, B. Mennucci, M. Cossi, G. Scalmani, N. Rega, G.A. Petersson, H. Nakatsuji, M. Hada, M. Ehara, K. Toyota, R. Fukuda, J. Hasegawa, M. Ishida, T. Nakajima, Y. Honda, O. Kitao, H. Nakai, M. Klene, X. Li, J.E. Knox, H.P. Hratchian, J. B. Cross, C. Adamo, J. Jaramillo, R. Gomperts, R.E. Stratmann, O. Yazyev, A.J. Austin, R. Cammi, C. Pomelli, J.W. Ochterski, P.Y. Ayala, K. Morokuma, G.A. Voth, P. Salvador, J.J. Dannenberg, V.G. Zakrzewski, S. Dapprich, A.D. Daniels, M.C. Strain, O. Farkas, D.K. Malick, A.D. Rabuck, K. Raghavachari, J.B. Foresman, J.V. Ortiz, Q. Cui, A. G. Baboul, S. Clifford, J. Cioslowski, B.B. Stefanov, G. Liu, A. Liashenko, P. Piskorz, I. Komaromi, R.L. Martin, D.J. Fox, T. Keith, M.A. Al-Laham, C.Y. Peng, A. Nanayakkara, M. Challacombe, P.M.W. Gill, B. Johnson, W. Chen, M.W. Wong, C. Gonzalez and J.A. Pople, *Gaussian 03, revision B.05*. (Gaussian, Inc., Pittsburgh, PA, 2003).
[75]C. Lee, E. Yang and R.G. Parr, Phys. Rev. B **37**, 785 (1988).
[76]A.D. McLean and G.S. Chandler, J. Chem. Phys. **72**, 5639 (1980).
[77]R. Krishnan, J.S. Binkley, R. Seeger and J.A. Pople, J. Chem. Phys. **72**, 650 (1980).
[78]D. Andrae, U. Haussermann, M. Dolg, H. Stoll and H. Preuss, Theor. Chim. Acta. **77**, 123 (1990).
[79]J.A. Pople, M.H. Gordon and K. Raghavachari, J. Chem. Phys. **87**, 5968 (1987).
[80]E. Broclawik, R. Yamauchi, A. Enduo, M. Kubo and A. Miyamoto, J. Chem. Phys. **104**, 4098 (1996).

[81]E. Broclawik, R. Yamauchi, A. Enduo, M. Kubo and A. Miyamoto, Int. J. Quantum Chem. **61**, 673 (1997).
[82]D.Y. Hwang and A.M. Mebel, Chem. Phys. Lett. **365**, 140 (2002).
[83]D.Y. Hwang and A.M. Mebel, J. Phys. Chem. A **106**, 12072 (2002).
[84]X. Xu, F. Faglioni and W.A. Goddard III, J. Phys. Chem. A **106**, 7171 (2002).
[85]G.J. Wang, M.H. Chen and M.F. Zhou, J. Phys. Chem. A **108**, 11273 (2004).
[86]G.J. Wang, S.X. Lai, M.H. Chen and M.F. Zhou, J. Phys. Chem. A **109**, 9514 (2005).
[87]G.J. Wang, Y. Gong, M.H. Chen and M.F. Zhou, J. Am. Chem. Soc. **128**, 5974 (2006).
[88]I. Bassi, G. Allegra, R. Scordamaglia and G. Chiccola, J. Am. Chem. Soc. **93**, 3787 (1971).
[89]R. Baumann, R. Stumpf, W.M. Davis, L.C. Liang and R.R. Schrock, J. Am. Chem. Soc. **121**, 7822 (1999).
[90]R.R. Schrock, Chem. Rev. **102**, 145 (2002).
[91]H.G. Cho and L. Andrews, J. Am. Chem. Soc. **126**, 10485 (2004).
[92]H.G. Cho and L. Andrews, J. Phys. Chem. A **108**, 6294 (2004).
[93]W. Scherer and G.S. McGrady, Angew. Chem. Int. Ed. **43**, 1782 (2004).
[94]M. Pettersson, E.M.S. Macoas, L. Khriachtchev, J. Lundell, R. Fausto and M. Rasanen, J. Chem. Phys. **117**, 9095 (2002).
[95]J. Espinosa-Garcia, J.C. Corchado and D.G. Truhlar, J. Am. Chem. Soc. **119**, 9891 (1997).
[96]Y.Y. Zhao, Y. Gong, M.H. Chen, M.F. Zhou and C.F. Ding, J. Phys. Chem. A **109**, 11765 (2005).
[97]Y.Y. Zhao, G.J. Wang, M.H. Chen and M.F. Zhou, J. Phys. Chem. A **109**, 6621 (2005).
[98]Y.Y. Zhao, Y. Gong, M.H. Chen and M.F. Zhou, J. Phys. Chem. A **110**, 1845 (2006).
[99]Y.Y. Zhao, Y. Gong and M.F. Zhou, J. Phys. Chem. A **110**, 10777 (2006).
[100]A.J. Merer, Ann. Rev. Phys. Chem. **40**, 407 (1989).
[101]L.N. Zhang, J. Dong and M.F. Zhou, J. Phys. Chem. A **104**, 8882 (2000).
[102]M.F. Zhou, L.N. Zhang, J. Dong and Q.Z. Qin, J. Am. Chem. Soc. **122**, 10680 (2000).
[103]M.F. Zhou, J. Dong, L.N. Zhang and Q.Z. Qin, J. Am. Chem. Soc. **123**, 135 (2001).
[104]M.F. Zhou, L.N. Zhang, L.M. Shao, W.N. Wang, K.N. Fan and Q.Z. Qin, J. Phys. Chem. A **105**, 5801 (2001).
[105]L.N. Zhang, M.F. Zhou, L.M. Shao, W.N. Wang, K.N. Fan and Q.Z. Qin, J. Phys. Chem. A **105**, 6998 (2001).
[106]J.W. Kauffman, R.H. Hauge and J.L. Margrave, J. Phys. Chem. **89**, 3541 (1985).
[107]M.H. Chen, H. Lu, J. Dong, L. Miao and M.F. Zhou, J. Phys. Chem. A **106**, 11456 (2002).
[108]M.F. Zhou, M.H. Chen, L.N. Zhang and H. Lu, J. Phys. Chem. A **106**, 9017 (2002).
[109]J.W. Kauffman, R.H. Hauge and J.L. Margrave, High. Temp. Sci. **17**, 237 (1984).
[110]J. Szczepanski, M. Szczesniak and M. Vala, Chem. Phys. Lett. **162**, 123 (1989).
[111]D.W. Ball, R.H. Hauge and J.L. Margrave, Inorg. Chem. **28**, 1599 (1989).
[112]M. Park, R.H. Hauge, Z.H. Kafafi and J.L. Margrave, J. Chem. Soc., Chem. Commun. 1570 (1985).
[113]G. Maier, H.P. Reisenauer and H. Egenolf, Monatshefte Fur Chemie **130**, 227 (1999).
[114]V.N. Khabashesku, K.N. Kudin, J.L. Margrave and L. Fredin, J. Organomet. Chem. **595**, 248 (2000).
[115]D.V. Lanzisera and L. Andrews, J. Phys. Chem. A **101**, 1482 (1997).
[116]Z.G. Huang, M.H. Chen, Q.N. Liu and M.F. Zhou, J. Phys. Chem. A **107**, 11380 (2003).
[117]Z.G. Huang, M.H. Chen and M.F. Zhou, J. Phys. Chem. A **108**, 3390 (2004).
[118]H.A. Joly, J.A. Howard and G.A. Arteca, Phys. Chem. Chem. Phys. **3**, 750 (2001).
[119]M.H. Chen, Z.G. Huang and M.F. Zhou, J. Phys. Chem. A **108**, 5950 (2004).
[120]G.J. Wang and M.F. Zhou, Ti, V, Cr, Mn, Fe + CH_3OH (unpublished).
[121]D. Schroder, S. Shaik and H. Schwarz, Acc. Chem. Res. **33**, 139 (2000).
[122]G.V. Chertihin and L. Andrews, J. Phys. Chem. **99**, 6356 (1995).